4298

office of
pipeline
safety

U.S. Department
of Transportation
Research and
Special Programs
Administration

Damage Assessment and Confinement in Offshore Pipelines

September 1982
DOT/RSPA/DMA-5018218

Final Report
Under Contract
DTRS5680-C-00010

Prepared by Office
of University Research

This document is available to the U S public through the National Technical Information Service, Springfield, Virginia 22161

NOTICE

This document is disseminated under the sponsorship of the Department of Transportation in the interest of information exchange. **The United States Government assumes no liability for its contents or use thereof.**

Technical Report Documentation Page

1. Report No.	2. Government Accession No.	3. Recipient's Cotolog No.
DOT-RSPA-DMA-50/82/8		

	5. Report Dote: February 1982
	6. Performing Organization Code
	8. Performing Organtzotion Report No.
	10. Work Unit No. (TRAIS)
	11. Contract or Grant No.: DTRS5680-C-00010
	13. Type of Report ond Period Covered: Final Report
	14. Sponsoring Agency Code: DMA-50

16. Abstract

This report presents the results of research on four problems of the propagating buckle in marine pipelines. Simulated accidental damage is produced in the laboratory on model pipes with point type and knife (line) type indentors. These damaged pipes are subjected to external pressure and a propagating buckle initiated. It is found that the point type and line type damage produce similar initiation pressures when the damage is characterized by the ovality of the most damaged section.

A propagating buckle can also be initiated from a bending buckle. Using model pipes, it is shown experimentally that bending of the pipe beyond that needed to buckle it does not have a large influence on the initiation pressure.

A propagating buckle can be conveniently arrested by using the so-called slip-on arrestor. In practice, this arrestor has a gap between the arrestor and the pipe which can considerably degrade the arrestor performance. It is shown that the loss in efficiency can be somewhat mitigated by the use of grout.

The propagating buckle can cause a fracture of .the pipeline due to the large strains that occur in the flattened pipe. An analysis is developed to determine the shape of the collapsing pipe and associated strains. Separate bend tests are conducted to determine the bend radius to produce fracture.

17. Key Words	18. Distribution Statement
Pipelines, Propagating Buckle, Buckle Arrestors, Pipe Fracture, Pipe Bending	Document is available to the U. S. public through the National Technical Information Service, Springfield, Virginia 22161

19. Security Classif. (of this report)	20. Security Classif. (of this page)	21. No. of Pages	22. Price
Unclassified	Unclassified		

METRIC CONVERSION FACTORS

Approximate Conversions to Metric Measures

Symbol	When You Know	Multiply by	To Find	Symbol
		LENGTH		
in	inches	*2.5	centimeters	cm
ft	feet	30	centimeters	cm
yd	yards	0.9	meters	m
mi	miles	1.6	kilometers	km
		AREA		
in^2	square inches	6.5	square centimeters	cm^2
ft^2	square feet	0.09	square meters	m^2
yd^2	square yards	0.8	square meters	m^2
mi^2	square miles	2.6	square kilometers	km^2
	acres	0.4	hectares	ha
		MASS (weight)		
oz	ounces	28	grams	g
lb	pounds	0.45	kilograms	kg
	short tons (2000 lb)	0.9	tonnes	t
		VOLUME		
tsp	teaspoons	5	milliliters	ml
Tbsp	tablespoons	15	milliliters	ml
fl oz	fluid ounces	30	milliliters	ml
c	cups	0.24	liters	l
pt	pints	0.47	liters	l
qt	quarts	0.95	liters	l
gal	gallons	3.8	liters	l
ft^3	cubic feet	0.03	cubic meters	m^3
yd^3	cubic yards	0.76	cubic meters	m^3
		TEMPERATURE (exact)		
°F	Fahrenheit temperature	5/9 (after subtracting 32)	Celsius temperature	°C

*1 in = 2.54 (exactly). For other exact conversions and more detailed tables, see NBS Misc. Publ. 286, Units of Weights and Measures, Price $2.25, SD Catalog No. C13.10:286.

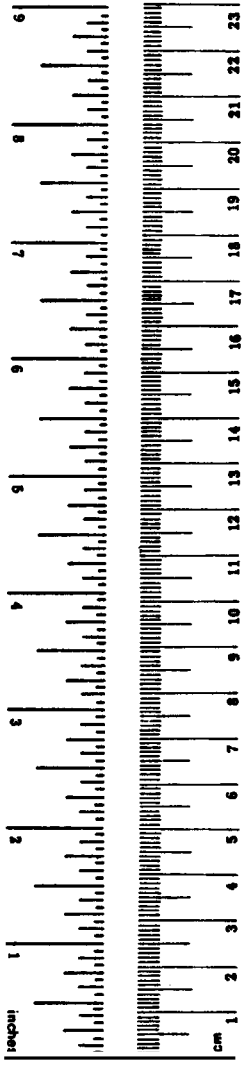

Approximate Conversions from Metric Measures

Symbol	When You Know	Multiply by	To Find	Symbol
		LENGTH		
mm	millimeters	0.04	inches	in
cm	centimeters	0.4	inches	in
m	meters	3.3	feet	ft
m	meters	1.1	yards	yd
km	kilometers	0.6	miles	mi
		AREA		
cm^2	square centimeters	0.16	square inches	in^2
m^2	square meters	1.2	square yards	yd^2
km^2	square kilometers	0.4	square miles	mi^2
ha	hectares (10,000 m^2)	2.5	acres	
		MASS (weight)		
g	grams	0.035	ounces	oz
kg	kilograms	2.2	pounds	lb
t	tonnes (1000 kg)	1.1	short tons	
		VOLUME		
ml	milliliters	0.03	fluid ounces	fl oz
l	liters	2.1	pints	pt
l	liters	1.06	quarts	qt
l	liters	0.26	gallons	gal
m^3	cubic meters	35	cubic feet	ft^3
m^3	cubic meters	1.3	cubic yards	yd^3
		TEMPERATURE (exact)		
°C	Celsius temperature	9/5 (then add 32)	Fahrenheit temperature	°F

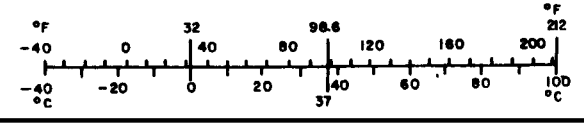

DAMAGE ASSESSMENT AND CONFINEMENT IN OFFSHORE PIPELINES

EXECUTIVE SUMMARY

This report presents the results of research carried out at the California Institute of Technology and the University of Texas at Austin. The subject of the research was problems of the propagating buckle in marine pipelines. This type of buckling is of concern during the construction and operation of undersea pipelines. It can result from construction mishaps or damage inflicted on an operational pipeline.

The report is divided into three sections. The first section discusses the conditions under which a propagating buckle can be initiated. Two specific conditions are considered: propagating buckle initiation from a localized damage to the pipeline and propagating buckle initiation due to a bending buckle. The second section discusses one method of arresting a propagating buckle once it has been initiated. This method is to place a larger pipe around the pipe and fill the gap between the two with a grout. This is known as the "slip-on" arrestor. The third section deals with the problem of pipe fracture due to a propagating buckle. This is sometimes referred to as the wet buckling problem.

The objectives of the research are to provide a fundamental understanding of the subject problems. This is achieved by carrying out experimental and analytical studies where appropriate. The experimental studies utilize model pipes and the results are reported in a form that can be transferred to full scale results through previously established scaling laws.

A propagating buckle can be initiated from a variety of accidental causes. The most common accidents are those occurring during the construction process and accidental damage to an operating pipeline. The latter accident usually

occurs due to anchors or objects falling off ships and platforms. This type of damage was chosen for the first study. Damage was produced in the laboratory on the model pipes with point type and knife (line) type indentors. These damaged pipes were subjected to external pressure and a propagating buckle initiated. It was found that the point type and line type damage produced similar initiation pressures, P_I , when the damage was characterized by the ovality of the most damaged section. In order to coalesce the data for scaling to full size pipe, the initiation pressure is related to the propagating pressure. Therefore, in order to determine the initiation pressure, the propagation pressure must be determined either from empirical equations or from tests, Knowing this and the character of the most damaged section, the initiation pressure can be found.

The experimental results of the work are presented in fig. 16. It should be noted that the data scatter is larger for slight damage than for large damage. Therefore, some conservativism is appropriate when using this part of the experimental results.

A propagating buckle can also be initiated from a bending buckle. This has been known from previous results, but the influence of the post buckled bend angle has not been studied. Using model pipes, it was shown experimentally that further bending of the pipe beyond that needed to buckle it did not have a large influence on the initiation pressure. The experimental results, fig. 32 and 33, show that further bending tends to increase the initiation pressure in most cases. Therefore, provided the pipe is not fractured during the bending process, the initiation pressure for slight post buckle bending is a reasonable lower bound of the initiation pressure.

A propagating buckle can be conveniently arrested by using the so called slip-on arrestor. In practice, this arrestor has a gap between the arrestor and the pipe, which is usually filled with a grout. It has been shown previously that an

unfilled gap can considerably degrade the performance of an arrestor. This performance (arrestor efficiency) has been determined empirically. The experimental work carried out (Ag. 41) shows that the loss in efficiency can be somewhat mitigated by the use of grout. The grouted arrestors, even with gaps as large as 8% of the radius, suffered a loss of only 25% of their no gap efficiency.

The propagating buckle can cause a fracture of the pipeline due to the large strains that occur in the flattened pipe. This in turn leads to flooding which can have serious consequences. This problem is studied by using an analytical approach. The analysis determined the shape of the collapsing pipe and associated strains. A separate bend test was conducted to determine the bend radius to produce fracture. For the particular steel studied, X-60, it was found that a buckle propagating at the propagation pressure did not produce a wet buckle. This conclusion can not be extended to higher pressures where the analysis is no longer applicable.

The results of the research work have provided unique data on four separate problems. In addition, experimental and analytical approaches to the problem areas have been established for other investigations, The results of this study and future studies will allow a more rational approach to the structural design, construction and operation of subsea pipelines.

TABLE OF CONTENTS

1. PROPAGATING BUCKLE INITIATION

In the design of an offshore pipeline, there are two buckling pressures that must be considered. The first is the classical buckling pressure, P_c, which is determined by considering the buckling of an infinitely long pipe under the action of uniform external pressure (Ref. 1). If the pipe has a large diameter-to-thickness ratio (D/t) and is relatively free of geometrical initial imperfections, this pressure is accurately given by

$$P_c = \frac{2}{1-\nu^2} E \left\{\frac{t}{D}\right\}^3 \qquad (1.1)$$

Corrections to this formula are available to take into account thick wall effects, initial out of roundness, plasticity, etc. (Ref. 2). However, these corrections do not change the basic nature of this buckling or collapse pressure.

The second pressure is known as the propagation pressure P_p (Ref. 3,4). This pressure is defined as the minimum pressure at which established buckle can be propagated along the pipe. In general, in order to find this pressure experimentally, the pressure must be raised above the propagation pressure to "initiate" a propagating buckle. Once .initiated, the buckle can be propagated at constant pressure along the pipeline.

The propagating pressure has only been determined empirically. Attempts to calculate this pressure using numerical approaches have not been successful, An analogue problem was solved in reference 5 to explore the influence of material properties on the propagation pressure.

The range of pressures between P_c and P_p is the subject of this part of the research work. It should be clear that if a pipe is 'perfect" it will collapse at P_c, suitably modified to account for thick wall and plasticity effects. If the pipe is damaged in a very specific manner, a buckle may be propagated along the pipe

at the propagation pressure, P_p. Any damage to the pipe between these two limits will lead to a propagating buckle at a pressure that is dependent upon the damage. At this critical pressure a propagating buckle will initiate from the damaged area. The Initiation Pressure, P_I, is therefore, defined as the pressure that will initiate a propagating buckle. This pressure is dependent upon the damage (i.e. initial imperfection) and must be characterized in terms of the parameters of the initial imperfection.

This type of characterization has not been attempted for the buckling of undersea pipelines. From an analysis standpoint, the problem involves large displacement, large strain, elastic plastic behavior. The parameters of the initial imperfection (damage) are also ill defined. For this reason it was decided to attempt a characterization experimentally for a special class of imperfections. The imperfections considered are ones that are thought to be reasonable based upon the survey of accidents involving undersea pipelines. For most of the accidents, the damage was caused by buckling due to bending or by localized impact.

The next two sections of this report will describe the experimental work carried out to determine the Initiation Pressure for these two specifIc types of imperfections. The conclusions drawn from this work must necessarily be limited to imperfections of these specific types.

1.1 Propagating Buckle Due to Localized Damage

This section is concerned with determining the initiation pressure for pipes that are locally damaged. This damage is assumed to occur from some object contacting the pipe. A typical example would be a piece of equipment which has been dropped overboard and then strikes an unburied pipeline. The variety of this type of damage is great and it seemed necessary to look at two extreme

types. For this purpose, the damage inflicted on the model pipes was produced by either a point type indentor or a knife edge indentor.

After the damage was inflicted on the pipe, careful measurements were taken in order to quantify the imperfection. Complete imperfection scans were carried out and the data recorded automatically. Next the pipes were buckled and the initiation pressure determined. The details of the experimental program and the data correlation are given in the next sections.

1.1.1 Experimental Procedure The pipes used for these experiments were made of steel. The bulk of the data was taken on model-size pipes with diameters ranging from 1.250 in to 1.500 in. Two tests were performed on larger diameter pipe to determine if any scaling problems existed. The steel used for the pipes was 1018 or 1010. The material properties of the steel were not directly measured. Instead, the propagation pressure of each pipe size was found experimentally and this quantity was used to correlate the data. This seemed preferable to the use of a defined yield stress and an empirical equation for the propagation pressure. The dimensions of the test pipes and the propagation pressure are given in Table I.

The damage was inflicted on the pipes using a knife edge type indentor or a point indentor. The point indentors are actually rods of different diameters varying from 1/4 in. to 5/8 in., the ends of which have been radiused. The different point indentors are shown in figure 1.The knife edge indentors likewise have finite radii which vary from 3/32 in. to 5/4 in. The range of indentors is shown in figure 2. The dimensions of the ten different indentors are given in Table II.

The pipes were damaged using a conventional testing machine. The point indentors were pushed normal to the pipe surface. Indention depth was varied

by controlling the displacement of the testing machine. A range of knife edge indentor damage is shown in figure 3. For the knife edge damage, the edge of the indentor was aligned normal to the pipe axis. Indentor depth was controlled in the same manner as for the point indentor. A range of pipe knife indentor damage is shown in fig. 4.

The character of the knife edge and point damage is dissimilar in the neighborhood of the indentor but has much of the same character otherwise. Use will be made of this similarity in the data correlation. A comparison of these two types of damage is shown in two views in Fig. 5.

Each pipe that was damaged and pressure tested to determine its initiation pressure was carefully measured to quantify its initial imperfection. The measurements were carried out using a scanning device constructed for this purpose. The device, shown in fig. 6, clamps the pipe in a vertical position. A rotating table revolves around the pipe clamping. The measuring transducer, an LVDT, is attached to the rotating table on a vertical slide. The slide and rotating table and displacement transducer comprise a cylindrical coordinate system. The pipe shape is then measured referenced to this coordinate system.

The LVDT was calibrated prior to measurements using a micrometer. The vertical position is adjusted by hand. Measurements were taken every 0.5 inches. The circumferential motion is hand provided and the circumferential position is read by a photo diode device indicating off a black and white tape. The tape can be seen in figure 6. The indicating device is also used to trigger the data acquisition system to record the data during each circumferential scan. Data points are taken at 102 locations during each circumferential scan.

The data acquisition system used in this experiment is shown in fig 7. The system can convert and store data at a rapid rate (40,000 data points per

second). The data acquisition calculator was also used to convert the voltage readings to displacements and plot the data in the form of contour plots. Several typical contours are shown in figures 8 tc 11. Figures 8 and 9 show the damage resulting from the point indentor. Each contour is displaced 0.5 inches in the axial direction from the previous contour. Knife edge damage is shown in fig. 10 and 11. The difference between the point and knife damage is evident in the vicinity of the contact area. Outside of the immediate region the damage is similar.

After the imperfections were measured, the pipes were buckled to determine their initiation pressures. The ends of the pipes were closed by end caps. The pipes were then placed in a pressure tank and pressurized with water. A constant volume test was achieved by using a piston type water pump. The buckling could be detected by the drop ob in pressure when the buckle began to propagate.

The propagating buckle which initiates from the local damage is the typical dog bone type buckle reported earlier (Ref. 4). A few diameters from the local damage it is impossible to detect the nature of the initial cause of the buckle. Two examples of propagation from a point and knife damage are shown in Fig. 12.

1.1.2 Data Correlation The initiation pressure tests provided 43 pipe tests for correlation. The information obtained consists of the initial pressure, the propagation pressure and the imperfection survey for each test pipe. The correlation problem is to somehow relate the initiation pressure to the damage. Unfortunately there does not exist an analysis to help in this correlation. It is necessary to use judgement and trial and error in carrying out the correlation.

The goal of the correlation is to provide a simple and reasonably accurate

relation between the initiation pressure and the parameters of the imperfection. The parameters of the imperfection are quite diverse. In addition, in a situation in practice, the amount of information about the damage would most likely be limited. It is, therefore, desirable to characterize the damage by the fewest number of parameters possible.

It is in this spirit that the characterization was undertaken. To begin with it was decided to find a relationship between the initiation pressure and the characteristics of the damage rather than the characteristics of the indentor. It seemed that the details of the damage should not be important. To illustrate this, several pipes of the same dimensions were damaged with approximately the same amount of damage by indentors of different diameters. The results of these tests are shown in figure 13 where the initiation pressure is shown as a function of the indentor diameter. The data are fairly independent of the indentor diameter with a slight decrease as the diameter increases. Some of this decrease can be explained by a closer examination of the damage (Table III), which shows that the pipes damaged with the larger indentors have somewhat larger damage. In any event, the data substantiates the hypotheses that the initiation pressure should not be a strong function of the indentor parameters, at least to the accuracy achievable in this correlation.

Next it was decided to attempt a data correlation based upon the parameters of the "most damaged" cross section of the pipe. This cross section was taken to be the cross section under the indentor. In most cases this cross section was visibly the most damaged.

Once this decision was made, the next problem was to somehow characterize this cross section. A typical cross section is given in fig. 14. Several parameters are obvious candidates for consideration. Among these are the maximum diameter, D_{max}, and the minimum diameter, D_{min}. Since the cross section is not

necessarily convex, these dimensions are defined as measured between parallel lines. In addition, the section may not have an axis of symmetry so that the D_{max} and D_{min} may not be at right angles to each other.

Other parameters that were tried in the correlation were the diameters of the circumscribed and inscribed Circles that have a common center and the area inside the contour. These parameters were not as successful in coalescing the data and will not be further discussed.

The correlation was achieved by plotting on log paper the initiation pressure as a function of the various parameters. This was done for the test data points for each pipe size in order to establish an adequate power law relation. If the correlation showed sufficient promise the remaining test points were similarly plotted and then a master curve of all data constructed.

The correlation parameter that appears most promising is the ratio of D_{min} to D_{max}. The data for pipe # 2 is shown in fig. 15 for both the knife edge and point indentors. It is seen from this figure that there appears to be very little difference in the data for the knife edge and point indentor damage when plotted against this parameter.. The overall correlation shows some scatter but the coalescence is reasonable.

The data is next plotted for all the families of pipes. In order to bring the various families into agreement, the initiation pressure is normalized by the propagation pressure. It was also found that a diameter-to-thickness ratio parameter used to shift the horizontal axis was helpful in correlation of the data. The improvement in this was slight and can not be substantiated by the narrow range of diameter-to-thickness tested. The data for all tests is shown in fig. 16. There is some scatter in the data but it appears reasonable for the type of problem considered.

In the spirit of seeking the fewest number of parameters for the correlation, the initiation pressure data are presented in flg. 17 as a function of the minimum diameter as divided by the original diameter. This correlation is not quite as good as the previous one but may be useful for some purposes. The data for the large diameter pipe (#4) are also given in this figure. The agreement with the small diameter pipe is reasonable although the large diameter results lie on the lower bound of the data. The propagating pressure for this pipe was calculated since it could not be measured in the initiation tests because the pipe fractured at the initiation pressure. Photographs of the propagated buckle and the fracture are shown in fig. 18. The fracture can be seen along the edge of the collapsed section of the pipe.

***1.1.3** Conclusions* The pressure at which a local damage initiates a propagating buckle has been studied experimentally. The local damaged area was produced by point and knife edge indentors of different diameters. It was shown that the diameter of the indentor did not have much influence on the value of the initiation pressure. Tests with pipes of different dimensions showed that the data could be successfully correlated using the propagating pressure to normalize the initiation pressure and characterizing the damaged area by the geometric properties of the most damaged section. The parameter that gave the best correlation was the minimum diameter divided by the maximum diameter which is a common measurement of out of roundness. For the application at hand the data are fairly well correlated for large out of roundness but considerable scatter exists for small out of roundness. Other simple correlations were attempted and one, minimum diameter divided by nominal diameter, was fairly successful.

Two tests of large diameter pipe were carried out of assess scale effects. No significant differences were noted in these tests as far as the initiation pressure

is concerned. It should, however, be emphasized that the present tests are confined to local damage. Tests of pipes with damaged areas that are elongated in the axial direction will produce lower initiation pressures.

12 Buckling Due to Bending and External Pressure

The implications of local dents on pipelines under external pressure were discussed in section 1.1. One of the other most common types of pipeline damage is bending buckles. These can be due to earthquakes, sediment instabilities, severe sea floor currents that tend to move the pipeline, anchors pulling on the pipeline, as well as buckles induced during the laying process. Since the pipe is under external pressure, such local damage can initiate a propagating buckle. The pressure at which a local damage transforms itself into the correct profile to become a propagating buckle is called the initiation pressure, P_I. Its value depends on the geometric characteristics of the dent. These include both the geometry as well as the amplitude of the damage. To establish these, it is necessary to find the conditions that lead to buckling and then to examine the post-buckling configuration that results.

Although a great deal of work has been done on pure bending as well as combined bending and external pressure of cylindrical shells [8-14], only relatively thin elastic structures have been considered ($D/t > 100$). For pipelines, the diameter to thickness range is $15 < D/t < 80$. For this range of D/t plastic effects are unavoidable. In what follows, the experimental equipment and methodology developed for studying the response, stability and post buckling behavior of pipes having D/t in the above range given are described. The response under combined bending and pressure is recorded, the point of instability established and the stability envelope as a function of both pressure and moment is obtained. In addition, the conditions under which a local buckle initiates a propagating one are studied for the two classes of damages identified in these

experiments.

1.2.1 Combined Loading Test Facility The experimental facility for the combined loading experiment was designed and built in house. It consists of a pure bending device which slides into a pressure tank and can be operated remotely while under external pressure (Fig. 19). Figure 20 shows a schematic representation of the bending device. Two pairs of sprockets, 9 in. in diameter, symmetrically placed 36 in. apart on a beam frame provide the bending moment. The distance that separates the two sets of sprockets can be varied so that different lengths of pipe can be tested. The sprockets support two rollers which apply point loads in the form of a couple at each end of the test specimen. Chains running over the sprockets are connected to a load cell and a hydraulic cylinder as shown in the figure.

Rotation of the sprockets can be achieved by contracting or extending the hydraulic cylinder. A hydraulic control system, which allows reversal of the flow, was designed and built in order to carefully control the movement of the cylinder. A load cell in series with the cylinder continuously monitors the tension in the chains. The applied moment can be found by multiplying the tension load by the sprocket radius.

The rotation of each sprocket is measured by an LVDT as follows. A thin steel cable runs over the hub of the sprocket and is in turn connected to the LVDT core. The LVDT is fixed at a position such that its axis is aligned with the horizontal tangent of the sprocket hub. Angular movement of the sprockets produces linear movement of the LVDT core. The cable is kept in tension by inserting a soft spring in series as shown in the figure. Each LVDT independently measures the rotation of each sprocket rotates. The two signals are electronically added and the resultant voltage is directly proportional to the curvature. (Note that this is a pure bending device so the curvature is constant across the length

of the test specimen.)

The load is transferred to the test specimen through two rollers that produce a couple on each end of the pipe. The rollers allow free horizontal movement of the test specimen. This is necessary in order to avoid axial loads in the pipe. The test specimen is closed at both ends by solid steel plugs as shown in *Fig.* 21. These plugs extend about 12 in. on either side of the pipe specimen so that the rollers are always in touch with the solid bars rather than the thin pipe. This was necessary in order to avoid loading the thin pipe directly through point loads which can prematurely cause local dimpling of the pipe. The end plugs were designed in such a way so as to reduce the stress concentration due to the discontinuity in the pipe cross section. The plug and pipe assembly is positioned in the device as shown in Fig. 19. Pipes having diameters from 0.75 - 1.5 in. and lengths from 25 - 50 in. can be tested.

The testing machine is capable of applying moments up to 10,000 in-lb. The whole apparatus was designed in a manner to ensure a "rigid" machine situation as far as the test specimen is concerned. This type of design is necessary in order to guarantee minimum effect from the testing machine on the pipe post-buckling configuration. The energy absorbed by the testing machine is less than 5% of the energy in the deformed pipe.

The whole device with the test specimen slides into a pressure tank. The tank has a diameter of 18 in., length of 8 ft. and working pressure of 800 psi. It can be pressurized by water or air or filled with water and pressurized with air. Each of the three pressurization methods establishes different experimental conditions. The bending device can be remotely controlled from outside the tank. The LVDT's and load cell are hermetically sealed and can operate under high pressure in water.

1.2.2 Experimental Procedure Two series of experiments were carried out. In both cases aluminum 6061-T6 tubes were used due to their availability in good quality. In the first series, the tubes had a nominal diameter, D, of 1.215 in. and thickness, t, of 0.035 in. and in the second series D= 0.980in. and t= 0.020 in. These two sizes were chosen because of the differences exhibited in their post-buckling behavior. All tubes tested had an effective length of 29 in.

The tubes were sealed on both sides using the long plugs described earlier (see Fig. 21). The ends of the plugs were epoxied to the tubes to ensure atmospheric internal pressure at all stages of the experiment. After positioning the pipe in the testing machine, the instruments were zeroed and the bending device was placed in the tank (see Fig. 19). As explained earlier, the tank can be pressurized in any of three different ways, each of which establishes different experimental conditions. For most experiments the tank was filled with water leaving an air pocket that was subsequently pressurized by air. This arrangement simulates a "nearly" constant pressure condition similar to the physical situation that the pipe encounters in the ocean. On buckling, the volume displaced by the pipe suddenly decreases and the air pocket expands to fill the extra volume generated. If the ratio of the volume of the air pocket to the volume generated by buckling is large enough, the pressure in the tank remains practically constant. On buckling under combined loading, a propagating buckle may be initiated from the resultant local damage. This must be determined without opening the tank so the following procedure was devised. As soon as buckling occurred (noise and sudden drop in the moment), loading was stopped and the pressure transducer output checked. The air pocket in the tank was arranged to be of such a size that if the local buckle propagated, collapsing the total length of the pipe, then the pressure in the tank would drop by 2-3 psi. Such a discontinuity in pressure can easily be observed on the pressure-time record kept during the

experiment. If such a step change was observed the experiment was considered completed. If not, the pressure was increased until a propagating buckle was finally initiated from the damaged section of the pipe.

For experiments where only the moment-curvature response was sought, the tank was completely filled and pressurized with water using a single piston pressure pump. The pressure tank and pressurization system are arranged in such a way so that the whole system can be vented and practically all the air bled out of the system. For pressures below 500 psi the volume expansion of the tank is negligible. The pipe specimen tested under such conditions sees a relatively rigid system. This was taken to represent a constant volume experimental condition. Any sudden change in the geometry of the pipe causes a drop in the pressure due to the relative stiffness of the loading system.

For all the experiments presented the following loading procedure was followed irrespective of the way the tank was pressurized. After positioning the testing machine and specimen in the tank, the system was pressurized to the required level and the pipe was subsequently deformed by rotating the sprockets. The sprocket rotation was manually controlled and was very slow. The process can be considered to be quasistatic. The pipe was continuously deformed until buckling occurred. The moment, curvature and pressure were recorded during the experiment on strip chart recorders. On buckling, the moment dropped drastically and the LVDT output increased suddenly. The LVDT's reading after buckling was used to approximately calculate the post-buckling configuration of the pipe.

1.2.3 Experimental Results A number of investigators, [13,14,15,16], have shown that there are two types of instability in the case of pure bending of a circular pipe. The first is a limit point type of geometric instability (i.e., $\frac{dM}{d\kappa} \to 0$)

and the second is a bifurcation type of instability typical of many thin structures under compressive stresses. Figure 22 shows a number of typical responses obtained from combined loading experiments on pipes with D/t = 34.7. For the case of zero pressure the response follows a linear path for low curvatures and as expected it becomes nonlinear for higher values of curvature. The maximum value of moment achieved appears to be a limit point. For external pressures higher than zero, the path is similar but buckling occurs much earlier. In these cases it is not possible to establish from the experimental results what type of instability occurred.

One way of physically looking at the interaction failure is as follows. By bending the pipe in a circular arc, the cross sections of the pipe tend to ovalize, which causes a reduction in the bending rigidity of the pipe. The application of an external pressure to such an ovalized pipe causes the already non-circular cross section to become more oval, which further reduces the bending rigidity of the pipe and eventually causes buckling under the applied moment.

The second mechanism involved can be described as follows. It has been shown in Ref. 5 that initial geometric imperfections in the cross section of an elastoplastic pipe will cause a reduction in its buckling pressure. The applied bending causes the cross sections to ovalize and when the ovalization reaches a critical value the pipe buckles under the external pressure. Clearly the two mechanisms interact. However, one can say that the first mechanism dominates for low pressures and the second one for pressures closer to the buckling pressure of a circular pipe.

The pressures at buckling, normalized by the buckling pressure of the pipe ($P_c = \frac{2E}{1-\nu^2}\left\{\frac{t}{D}\right\}^3$), are plotted vs. the moment at buckling normalized by the elastic limit load ($M_m^e = .987\frac{E}{\sqrt{1-\nu^2}}Rt^2$) for the two different D/t in Figures 23 and 24

The corresponding pressure-curvature plots are shown in Figures 25 and 28. A limit type load analysis carried out recently in [17] found the experimental results for D/t = 34.7 to be in good agreement with the predicted limit loads. On the other hand for D/t =49.0, considerable difference was observed particularly in the case of the pressure-curvature interaction plot. This reinforces the earlier expressed opinion that the thinner pipes exhibited bifurcation failure before the limit load was reached. Due to the features of the $M-\kappa$ curves for higher values of curvature, bifurcation does not cause a pronounced reduction of the values of moment predicted by the limit load analysis. The limit and bifurcation values of curvature however, can be substantially different. The buckles that initiated a propagating buckle are indicated on all figures. The initiation pressure for dents caused by local buckling under combined loading is clearly very close to the pipe propagation pressure in both cases. This contradicts efforts by previous investigators [3] to define the initiation pressure as another characteristic pressure of the pipe.

Figures 27 and 26 show two typical buckles obtained by pure bending of the pipes for the two D/t ratios considered. The difference in the mode of buckling is obvious. For D/t = 34.7 a single crosswise dent occurs. The damage is restricted to about 5 diameters on either side of the dent. The geometry of the damage is doubly symmetric. For D/t = 49.0 the pipe buckles in a diamond mode typical of buckling of elastic shells under axial load. The buckle affects a smaller length of pipe and has only one plane of symmetry. This difference in behavior has consistently been observed in pipes of other sizes as well (e.g., D/t = 32.1 and 68.7). Further experiments are necessary in order to establish the exact D/t at which the mode changes.

The difference in the mode of failure seems to also affect the initiation pressure of the buckled pipes. As mentioned in the introduction, it was felt that the

initiation pressure should be a function of the type of damage inflicted to the pipe as well as its severity. The buckle usually propagates in a dog bone type of collapse so that any damage that tends to easily progress to that mode will have a low initiation pressure.

In an effort to establish a parameter that measures the amplitude of the damage for different pipes, the angle ϑ_c was chosen (this angle is defined in Figure 32). Pipes bent to different values of ϑ_c are shown in Figure 29. A series of experiments was carried out for pipes having $D/t = 49.0$ and 34.7 where the initiation pressure was found as a function of the post-buckling angle ϑ_c. Each pipe was first buckled under pure bending. By further rotating the sprockets the required angle ϑ_c was established. The bending device was subsequently locked in that position and placed into the pressure tank. The experiments were carried out under constant pressure conditions. The pressure was increased until a propagating buckle was initiated. Fig. 30 shows a buckle initiated from such damage. For the bigger values of ϑ_c the damaged pipe locally buckled under pressure without propagating (see Fig. 31). In such cases pressurization was continued until the buckle finally propagated.

The results of these experiments are shown in Fig. 32 and 33. For $D/t = 34.7$ the initiation pressure increases with ϑ_c. For the smallest buckling angle obtained ($\vartheta_c = 4.5^0$), $P_I = 1.17P_p$. The results can be fitted with a smooth curve. For $D/t = 49.0$, the results show more scatter. If any conclusion can be drawn in this case, it is that the buckling angle ϑ_c is not one of the parameters that significantly affect the initiation pressure. This can be expected because the geometry of the damage varies much more from pipe to pipe than in the case of $D/t = 34.7$. However, the lowest initiation pressure obtained in this case was $P_I = 1.49P_p$. This indicates that for more irregular and complex post-buckling configurations, the propagating buckle is more difficult to initiate.

1.2.4 Conclusion Combined pressure-moment buckling tests have been carried out for pipes with two different diameter-to-thickness ratios. The buckling behavior varies from a limit type buckling to a bifurcation type buckling, The failure mode changes along the interaction envelope. For low pressure and high moment, the failure mode is a local dent. For pressures somewhat higher than the propagation pressure, the failure mode includes a complete collapse of the pipe. This transition point is higher than the propagation pressure but the difference is not as great as that reported by previous investigators. The influence of post buckled configuration on this transition pressure was further studied. It was shown that the post buckling bend angle was not highly influential in the determination of the initiation pressure.

2. PROPAGATING BUCKLE ARREST

All subjects discussed so far have a diagnostic nature with the purpose of better understanding the problems involved in pipeline design. Looking at the problem from a different point of view, if a propagating buckle occurs the damage caused should be restricted to as small a pipeline section as possible. This is achieved by the proper use of buckle arrestors. These are devices which locally reinforce the pipe and prevent the buckle from propagating any further. They are installed at regular intervals l, along the pipeline thus restricting the damage to a maximum length l (Fig. 34).

A number of arresting devices have been suggested to date. Reference [18] describes devices which are temporarily placed on the inside of the pipe to locally prevent circumferential deformation. References [19-23] describe devices which are permanently placed on the outside of the pipe (Fig. 35). These are further discussed in [22 and 23].

The problem of efficiently designing these devices was addressed in detail in [22]. An experimental methodology and data reduction was developed and used to study the parametric dependence of the efficiency of the "slip-on" and "spiral" arrestors. Extensive experimental work was carried out and empirical relationships for the efficiencies of these devices were obtained as a function of the geometric and material parameters of the arrestors and pipes.

Perhaps the most favored of the arresting devices is the so called "slip-on" arrestor. This is a tight fitting ring which locally reinforces the pipe thus arresting a propagating buckle. Such a device is shown in flg. 36. Because pipes used for pipeline applications are inherently geometrically imperfect, it is very difficult in practice to achieve the close contact between the pipe and the arrestor required by the above idealization. In practical pipeline applications [24],

this problem is dealt with by filling the gap between the two surfaces with grout. This is usually a mixture of cement and tar or sand and epoxy. Inspite of the wide use of the above device, no systematic testing of this more complicated configuration has been carried out. In what follows the experimental effort started earlier on the "slip-on" arrestor is continued and extended to examine the effectiveness, if any, the grout has on the efficiency of such arresting devices.

2.1 Problem Description

The goal of a properly designed arrestor is to locally reinforce the pipe such that a dynamically propagating buckle is arrested. The parameters of the problem are shown in **fig. 37,** The pipe is characterized by two critical pressures.

(a) ***Propagation Pressure*** (P_p). This is defined as the lowest pressure which will sustain a propagating buckle. An empirical expression for this quantity derived in [22] is given by

$$\frac{P_p}{\sigma_0} = [10.7 + 0.54(\frac{\bar{E}}{\sigma_0})]\left\{\frac{t}{D}\right\}^{2.25} \qquad (2.1)$$

(b) ***Buckling Pressure*** (P_c) This is deflned as the pressure at which a long pipe under external pressure bifurcates. For buckling in the elastic regime

$$P_c = \frac{2E}{(1-\nu^2)}\left\{\frac{t}{D}\right\}^3 \qquad (2.2)$$

(c) *Crossover Pressure* (P_0) The combined assembly of the pipe and arrestor are characterized by the so called crossover pressure. This is deffined as the pressure at which an incoming buckle penetrates the arrestor.

Using these three critical pressures an arrestor efficiency (η) can be deflned as follows.

$$\eta = \frac{P_0 / P_p - 1}{P_c / P_p - 1} \tag{2.3}$$

Thus an arrestor which allows a propagating buckle to penetrate at P_p has an efacience 0; one that has a crossover pressure equal to P_c has an efficiency of 1.0.

The problem of finding the efficiency from experiments is quite complex due to the large number of parameters. Certain parameters are not important (i.e. Young's Modulus E in the expression for P_p) and the number of experiments can be simplified using this information.

For the slip-on arrestor a series of experiments were carried out [22] and the data correlated as shown in fig. 38. The arrestor efaciency then becomes

$$\eta = \frac{1}{43}\left(\frac{\sigma_0'}{\sigma_0}\right)\left(\frac{t}{D}\right)\left\{\frac{L}{t}\right\}^{3/2}\left\{\frac{h}{t}\right\}^{3} \tag{2.4}$$

Expression (6) resulted from a quasistatic examination of the arrest process. Additional experiments were carried out under dynamic arrest conditions (i.e. where the buckle was travelling at a velocity U). A comparison of the arrestor efficiencies under quasistatic and dynamic conditions are shown in fig.39. The efficiencies of the arrestors under quasistatic conditions were found to be lower than those under comparable dynamic conditions. Thus expression (6) is a conservative estimate of the actual efficiency.

2.2 ExperimentalProgram

Any gap between the pipe and arrestor can cause a substantial decrease in the crossover pressure of the arrestor. A series of experiments were carried out to measure this decrease [22]. The results are shown if flg. 40. Five different arrestor efficiencies were used in the test. The presence of the gap caused a reduction in the arrestor efficiency in all cases. The reduction was more pronounced in the case of the higher efficiency arrestors.

Tests were carried out to examine if grouting could reduce the negative effect of the gap on the efficiency. Arrestors having zero gap efaciencies of 0.77 and 1.0 were selected for these experiments. Two sets of tests were carried out for each efficiency. In the first set the gap size was varied with no grout. In the second set the arrestors were grouted. Plaster of Paris was used as a grout in all experiments. This was selected because of its relatively short setting time and the material stability in water. The two sets of results for the two groups of arrestors are shown in fig. 41. The grouted arrestors had a substantially improved performance compared to the ungrouted ones. In a few cases the efficiency of the grouted arrestors approached the efficiency at zero gap for that geometry. The observed experimental scatter can be attributed to uncontrolled factors like uneven distribution of grout, air bubbles in the grout, eccentric positioning of the arrestor etc. All of these experimental difficulties can be overcome in an industrial situation where the pipe dimension is larger and the whole process is automated.

Three dynamic experiments were also carried out to compare the dynamic and quasistatic arrestor efficiencies. Like in the case of the "slip-on" and "spiral" arrestors the dynamic effects caused an increase in arrestor efaciency.

23 CONCLUSION

Tests were conducted on slip-on arrestors with two different efficiencies to determine the influence of grouting the gap between arrestor and the pipe. The results show that the grout considerable improves the arrestor performance although it does not bring it up to that for an arrestor without a gap. For high efaciency arrestors the grout plays an important roll since the efficiency is greatly degraded by the existence of a gap as large as 1% of the diameter.

The tests were limited to one type of grout (plaster of Paris) and extrapola-

tion of the data to other cases should be done with caution. The effect of grout material properties such as brittleness, hygroelastic behavior etc. are not known at this time. The grout used did not bond to the pipe so that it acts largely in compression. Bonded arrestors may exhibit different characteristics particularly in the dynamic arrest condition. Dynamic tests conducted for the grouted arrestor show the same increase in efficiency as previously found for the ungrouted slip-on-arrestor.

3. WET BUCKLING

The wet buckle is the name given to any kind of severe damage which has caused rupture that leads to flooding of the pipeline. During laying, flooding will usually result in breaking of the pipeline due to the loss of buoyancy. The result is that one end of the open pipeline finds itself on the sea floor causing it to be filled up with sea bottom material. Walker, in ref. 25, mentions that in one such 'Incident", during the laying of the Fortier field pipeline, 6000 cu. ft. of dirt filled up the pipeline. It is very clear that the dewatering and cleaning up processes are very time consuming and consequently very costly. As a result, wet buckles, whatever their causes, are very undesirable.

There exist a number of causes of wet buckles. Some of these are predictable. This paper deals with the prediction of a wet buckle resulting from a propagating buckle. Figure 42 shows a picture of a buckle that propagated and stopped. The cross section collapses to a characteristic dog- bone shape. It is clear that four points on the cross section, symmetrically placed, undergo rather severe rotations during the collapse process. With the right combination of material properties and geometric characteristics of the pipe, this can result in local strains that exceed the ultimate strain of the pipe material. This leads to local material failure and rupture of the pipe thus creating a wet buckle. Figure 43 shows an example of a wet buckle which resulted from a propagating buckle.

It has been shown *[5]* that the areas that undergo maximum strain are the ones around the two points on the cross section which, on collapse, end up furthest apart. The local strain is a direct function of the local curvature (inextensionality of the cross section has been shown to be a reasonable assumption for $D/t > 30$). The magnitude of the curvature at these points depends flrst on the pressure at which propagation occurred, second on the geometric characteristics of the pipe (diameter D and thickness t), and third on the material

properties of the pipe.

As explained in ref. 21, buckle propagation can occur for pressures ranging between the propagation pressure (P_p) and the buckling pressure (P_c) of the pipe. An empirical expression for the propagation pressure obtained by the authors [4] is given by

$$P_p=\sigma_o\left[10.7+0.54\left\{\frac{E'}{\sigma_o}\right\} \right] \left\{\frac{t}{D}\right\}^{2.25} \tag{3.1}$$

For pipes that buckle in the elastic regime, the buckling pressure is given by

$$P_c = 2\ \frac{E}{1-\nu^2}\left\{\frac{t}{D}\right\}^3 \tag{3.2}$$

For realistic material properties and pipe dimensions, P_c is more than twice P_p. The dependence of the severity of deformation on pressure can be seen in fig. 44. It is important to note how the radius of curvature at the two extremes of the cross section gets progressively smaller as the pressure of propagation is increased from P_p to P_c.

It is clear that the problem involves large plastic deformations and for the most severely deformed cases large strains, even though these may be restricted to only the extreme ends of the cross section. For higher pressures, when parts of the two opposite walls begin to come into contact, elastic unloading occurs in some areas. As a result, deformation-type plasticity theory cannot be used.

A good approximation of the problem can be made by considering the problem to be two dimensional, i.e. considering only deformations of the cross section. A good model of the problem should consider the complete collapse of the cross section from a circular one to the configuration where the first two diametrically opposite points touch. This has been shown to be a good approximation for a buckle traveling at the propagation pressure [5]. For higher pres-

sures, parts of the cross section wall come into contact and deformation is restricted to the remainder of the contour. The deformation should be followed by varying the pressure until it reaches the value P_c. Any further increase in pressure is strictly of academic interest. Figure 45 shows a schematic representation of a typical load-displacement curve of a collapsing ring. During the deformation process, the strains at the points of minimum curvature should be carefully monitored to detect failure.

Clearly the problem is quite complex; as a result, it is being treated in three stages. This report includes the first stage of the analysis of the problem. The cross section is considered to be inextensional. An elastoplastic, large deformation analysis is used in order to follow the deformations of the collapsing ring. The configuration where the first two diametrically opposite points touch represents a buckle propagating at the propagation pressure. By examining the points of minimum curvature, one can decide whether a wet buckle is a possibility or not at a pressure equal to P_c. This can be done for different materials in order to test their suitability for use in pipelaying applications.

The second stage of the analysis - not reported here - will examine what happens after contact between the walls is established. The third stage will include large strains for more realistic modelling.

3.1 Problem Formulation

Consider a circular ring of radius R and thickness t, as shown in flg. 46. The ring can have an initial imperfection. For convenience this will be taken to be of the form

$$w_i = w_o \cos 2\vartheta \qquad (3.3)$$

The ring's midsurface is assumed to be inextensional.

Equilibrium Equations

The nonlinear equilibrium equations can be obtained by considering an elemental segment of the ring as shown in fig. 46b.

$$\frac{dH}{dS} = -P \cos \vartheta$$

$$\frac{dV}{dS} = -P \sin \vartheta, \tag{3.4}$$

$$\frac{dM}{dS} = H \cos \vartheta + V \sin \vartheta$$

H and V are the horizontal and vertical forces whereas M is the moment as deflned by flg. 46b. S is the coordinate along the midsurface of the ring and ϑ is the angle between the normal and the x-axis.

Geometry

Only inextensional deformations of the ring will be considered. As a result

$$\frac{dx}{dS} = -\sin \vartheta,$$

$$\frac{dy}{dS} = \cos \vartheta, \tag{3.5}$$

where (x,y) defines a point on the deformed ring relative to the Cartesian frame shown in fig. 46a.

Constitutive Behavior

Figure 47 shows the stress-strain relationship used. It was obtained from a longitudinal tension test carried out on an X-60 grade steel specimen cut along a line perpendicular to the axis of a 30 in. diameter, 0.562 in. thick pipe. The material is assumed to behave in the same way in compression. The moment (M) curvature (κ) relationship is obtained as follows

$$M=2\int_0^{t\kappa/2}\frac{1}{\kappa^2}\sigma(\varepsilon)\,\varepsilon\,d\varepsilon \qquad (3.6)$$

where

$$\kappa=\frac{d\vartheta_o}{dS}-\frac{d\vartheta}{dS}$$

and $\frac{d\vartheta_o}{dS}$ is the initial curvature.

The stress-strain relation was digitized appropriately and expression (3.6) is found by numerical integration. Figure 48 shows the results of this integration normalized appropriately. Let

$$K=\frac{\kappa}{\kappa_o}$$

where

$$\kappa_o=\frac{\varepsilon_o}{2t,} \qquad (3.7)$$

$$E,=0.005;$$

and

$$\bar{M}=\frac{M}{M_o}$$

where

$$M_o=\frac{\sigma_o t^2}{6,}$$

$$\sigma_o=\left\{\sigma \mid \varepsilon=\varepsilon_o\right\}$$

Then

$$\bar{M}=\bar{M}(K)$$

or

$$K = K(\bar{M}) \tag{3.8}$$

Non-dimensionalizing equations (3.4) appropriately, one obtains:

$$\frac{d\bar{H}}{ds} = -Q\cos\vartheta,$$

$$\frac{d\bar{V}}{ds} = -Q\sin\vartheta,$$

$$\frac{d\bar{M}}{ds} = \bar{H}\cos\vartheta + \bar{V}\sin\vartheta,$$

$$\frac{d\vartheta}{ds} = \frac{d\vartheta_0}{ds} - \frac{1}{\pi}\left\{\frac{R}{t}\right\} t\,\varepsilon_0\,K(\bar{M}) \tag{3.9}$$

The boundary conditions are:

$$\bar{H}(0) = 0,$$

$$\vartheta(0) = 0,$$

$$\vartheta(1) = \pi/2,$$

$$\bar{V}(1) = 0$$

In addition (3.5) becomes

$$\frac{d\bar{x}}{ds} = -\sin^*,\quad \bar{x}(1) = 0,\quad 0 \le s \le 1$$

$$\frac{d\bar{y}}{ds} = \cos\vartheta,\quad \bar{y}(0) = 0, \tag{3.10}$$

where

$$s = 2S/\pi R,\ \bar{x} = 2x/\pi R,\ \bar{y} = 2y/\pi R \tag{3.11}$$

$$\bar{M} = 6M/\sigma_0 t^2$$

$$\bar{H} = 3\pi\, HR/\sigma_o\, t^2$$

$$\bar{V} = 3\pi VR/\sigma_o\, t^2$$

$$Q = \frac{3}{2}\pi^2 \left\{\frac{R}{t}\right\}^2 \frac{P}{\sigma_o}$$

(3.9) can be expressed in vector form as:

$$\frac{d\underline{u}}{ds} = \underline{f}(s,\underline{u}) \tag{3.12}$$

$$\underline{u} = (\bar{H}\,,\ \bar{V}\,,\ \bar{M}\,,\ \vartheta)$$

$$u_1\,(0) = 0\ ,\ u_2\,(1) = 0,$$

$$u_3(0) = 0\ ,\ u_4\,(1) = \pi/2$$

Equations **(3.12)** describe a set of four nonlinear ordinary differential equations in the form of a two-point boundary value problem Newton's iterative numerical method is used to solve for $\underline{u}$. The interval $s \in [0,1]$ is divided into N discrete points where 264 $N \leq 50$, depending on the situation.

The convergence criterion used was as follows:

$$\max \left| u_j^{(\nu+1)} - u_j^{(\nu)} \right| \leq 10^{-4}$$

The numerical method used is described in more detail in ref. 26. The solution of the elastic small deformation linearized problem was used as initial guess, $\underline{u}^{(o)}$, to start the iteration. Then the parameter Q was increased by A Q and the solution at Q was used as an initial guess for Q + A Q.

For each point, $G(\bar{M})$ and $G'(\bar{M})$ were found by first interpolating around the specific value of $\bar{M}$ and then differentiating numerically. A six point divided difference interpolating algorithm was used.

In problems of this type, where elastoplastic material behavior is used, the

pressure-displacement response, at any point, develops a distinct limit point beyond which the ring (pipe) becomes unstable. For a pressure controlled problem (pressure increments ΔQ), the numerical procedure had difficulty converging for points around the limit point. Arbocz, in ref. 27, facing the same problem, but using the double shooting technique, successfully modified the equations so that increments of deformation were prescribed instead of load. This enabled the extension of the curve beyond the limit point. The same idea is used in this case but a different constraint is used.

From (3.5)

$$\frac{d\bar{y}}{ds} = \cos\vartheta, \quad \bar{y}(0) = 0$$

Suppose the constraint added is: $\bar{y}(1)=\Delta$, where Δ is to be prescribed each time.

Since displacement cannot be prescribed simultaneously with traction at a point, Q is treated as a new unknown to the problem. Since Q = const.

$$\frac{dQ}{ds} = 0$$

Equations (2.9) then become

$$\frac{d\bar{H}}{ds} = Q\cos\vartheta \tag{3.13}$$

$$\frac{d\bar{V}}{ds} = -Q\sin\vartheta, \quad 0 \le s \le 1$$

$$\frac{d\bar{M}}{ds} = -\bar{H}\sin\vartheta + \bar{V}\cos\vartheta$$

$$\frac{d\vartheta}{ds} = \frac{d\vartheta_0}{ds} - \pi\left\{\frac{R}{t}\right\}\varepsilon_0 K(\bar{M}),$$

$$\frac{d\bar{y}}{ds} = \cos\vartheta$$

$$\frac{dQ}{ds}=0,$$

with boundary conditions

$$\bar{H}(0) = 0$$

$$\vartheta(0) = 0$$

$$\vartheta(1) = \pi/2$$

$$\bar{V}(1) = 0$$

$$\bar{y}(0) = 0$$

$$\bar{y}(1) = \Delta \text{ (A prescribed for each calculation).}$$

In addition

$$\frac{d\bar{x}}{ds} = -\sin\vartheta, \qquad x(1) = 0. \tag{3.14}$$

The calculation proceeds in two stages. Using increments of Q, i.e. eqns. (3.9), the pressure was increased to a small distance below the limit point. The last converged solution was used as an initial guess for the next calculation where increments of displacement A were prescribed. Increments of displacement were used until complete collapse of the ring, Collapse condition, for the purposes of this exercise, was defined as the configuration in which the flrst two diametrically opposite points come into contact. Figure 49 shows a collapsing sequence, as obtained by the numerical solution of the problem, starting from n almost circular ring to one which is collapsed.

32 Results and Discussion

The purpose of this program was to develop a method for obtaining the value of the minimum curvature of the cross section of the pipe in the collapsed configuration. This was achieved by treating the nonlinear problem numerically.

Figure 49 shows the collapsing sequence of a pipe. develops. Figure 50 shows how the moment distribution varies along the ring perimeter on collapse. As expected, the maximum moment (and curvature) occurs at s=0. Figure 51 shows how the value of the moment at s=0 varies during the collapse process. It is very clear that no unloading occurs at any instance during collapse. This happens to be true for the whole cross section; as a result, the deformation theory of plasticity used more than suffices.

Figure 52 shows the pressure-displacement curve for the ring during the deformation process. A distinct limit point exists beyond which the path becomes unstable. The maximum pressure achieved in this curve is considered to be the buckling pressure of the ring. It should be noted that a small initial imperfection of the ring, of the type described by (3.3), was included in the analysis. The buckling pressure was shown to be sensitive to the value of this initial imperfection in Ref. 5.

The lowest pressure reached in the post-buckling regime is associated with the propagation pressure of the pipe [5]. For most realistic pipe material and geometric parameters, the lowest pressure occurs on collapse, This is true for the case examined in this report.

For a small area around s=0 and s=1, strains larger than 10%were calculated. The experimentally obtained stress-strain curve used (fig. 47) was restricted to 9%strain; the problem was solved by linearly extrapolating the existing curve to accommodate the demands of the problem. It is clear that at least for the latter part of the collapse process, the small strain assumption of the theory used was locally violated around s=0 and s=1. The extent of this error will be considered in the third stage of this effort.

Having obtained the minimum radius of curvature on collapse, a test was car-

ried out to flnd out whether the material would fail under such deformations. A strip of the same material as the one used for the analysis, having the correct thickness, was bent over a circular rod which had a radius equal to the minimum radius of curvature calculated. The cases tested were as follows:

Material: x-60 Grade Steel

σ_o = 56,000 psi

E = 30x10^6 psi

Ring Geometry: $\frac{R}{t}$ = 17.86

Maximum Curvature (nondimensional): G = 48.32

This implies: (a) for t= 0.050 in., Minimum Radius of Curvature = 0.414 in.; (b) for t= 0.040in., Minimum Radius Curvature = 0.331 in.

Both of the above cases were tested for failure. No failure occurred. It is thus concluded that a buckle propagating at the propagation pressure will not result in a wet buckle. No prediction can be made yet about what happens at higher pressures. It must also be noted that this prediction is restricted to the material considered. In fact, as already shown by the authors in ref. 4, the post-yield slope of the stress-strain curve very much affects the minimum radius of curvature obtained on collapse. This can be seen in Figure 12 where collapsed configurations are presented obtained from an analysis approximating the stress-strain behavior with a bilinear fit. The preyield characteristics of the material were kept constant and only the post-yield slope was varied. Clearly, for "softer" materials a smaller radius of curvature is obtained. This suggests that each material has to be treated separately.

33 Conclusion

The first stage of a study of wet buckles arising from propagating buckles has been presented. The method uses realistic stress-strain curves of pipeline materials in order to solve the problem of the collapse of a circular ring under external pressure. The minimum calculated curvature on collapse is used in order to carry out a separate test on a strip of the same material to find out whether such a curvature caused failure of the material.

REFERENCES

1. Timoshenko, S.P., Gere, J.M., **Theory of Elastic Stability**, McGraw-Hill, **1961.**

2. API Bulletin on Performance Properties of Casing, Tubing and Drill Pipe, **API** Bulletin C **52, 12th** Edition, April **1970.**

3. Mesloh, **R.,** Johns, T.G., Sorenson, **J.E.,** The Propagating Buckle," Proceedings, BOSS **76,** pp. **787-797,** Norway, **1976.**

4. Kyriakides, **S.** and Babcock, C.D., 'Experimental Determination of the Propagation Pressure of Circular Pipes," Journal of Pressure Vessel Technology, Trans. of the ASME, Vol. **103, Nov.** 1981, p. **326-336.**

5. Kyriakides, S., and Babcock, C.D., 'Large Deflection Collapse Analysis of an Inelastic Inextensional Ring Under External Pressure," International Journal of Solids and Structures, Vol. 17, No. 10, pp. **961-993,** 1981.

6. Brazier, **L.G.,** "On the Flexture of Thin Cylindrical Shells and Other 'Thin" Sections," Proc. Royal Society Series A, Vol. **106,** pp. 104-114, **(1927).**

7. Reissner, E., "On Finite Pure Bending of Cylindrical Tubes," Osterr. Ing. Arch., Vol. **15,** pp. **161-172, (1961)**

8. Reissner, E. and Weinitschke, H.J., "Finite Pure Bending of Cylindrical Tubes," Quart. of Appl. Math., Vol. **20,** pp. **305-319, (1963).**

9. Kogakushi, K.I., "Failure of Thin Circular Tubes Under Combined Bending and Internal or External Pressure," J. of Japanese Society of Aerospace Engineers, Vol. **7,** pp. **1109-1121,** Dec. **1940.**

10. Seide, P. and Weingarten, V.I., "On the Buckling of Circular Cylindrical Shells Under Pure Bending," J. of Appl. Mech., Vol. **26,** pp. **112-116, (1961).**

11. Stephens, V.B., Starnes, **J.H.** and Almroth, B.O., 'Collapse of Long Cylindrical Shells Under Combined Bending and Pressure Loads," AIM Journal, Vol. **13,**

pp. 20-25, (1975).

12. Axelrad, E.L., "Refinement of Critical Load Analysis for the Tube Flexure by Way of Considering Precritical Deformation," Izv. An SSSR, ONT, Mech.: Mash. n. 4 p. 123-129, (1965) (in Russian).

13. Axelrad, E.L., "Flexible Shells," Proceedings 15th IUTAM, Aug. 17-23, 1980, Toronto, Canada, pp. 45-56.

14. Fabian, O., "Collapse of Cylindrical, Elastic Tubes Under Combined Bending; Pressure and Axial Loads," Int. J. of Solids and Structures, Vol. 13, p. 1257-1270 (1977).

15. Tuggu, P. and Schroeder, J., "Plastic Deformation and Stability of Pipes Exposed to External Couples," Int. J. of Solids and Structures, Vol. 15, pp. 643-658,)1979).

16. Gellin, S., "The Plastic Buckling of Long Cylindrical Shells Under Pure Bending," Int. J. of Solids and Structures, Vol. 16, pp. 397-407, (1979).

17. Kyriakides, S., and Shaw, P.K., "!Response and Stability of Elastoplastic Circular Pipes Under Combined Bending and External Pressure," Proceedings of the 5th Annual Energy-Sources Technology Conf., ASME, March 7-10, 1982.

18. Lochridge, J.C., and Gibson, T.L., "Method of Arresting the Propagation of a Buckle in a Pipeline," U S. Patent 3,747,356, July 24, 1973.

19. Broussard, D.E., Ayers, R.R., and Walker, G.E., Jr., "Mitigation of Propagating Collapse Failures in Pipelines Due to External Load," U.S. Patent 3,768,269, October 30, 1973.

20. Johns, T.G. Mesloh, R.E., and Sorenson, J.E., "Propagating Buckle Arrestors for Offshore Pipelines," OTC 2680, May 1976.

21. Kyriakides, S., and Babcock, C.D., "On the Dynamics and the Arrest of the Propagating Buckle in Offshore Pipelines," OTC 3479, May 1979.

22. Kyriakides, S., and Babcock, C.D., "On the Slip-On Buckle Arrestor for Offshore Pipelines," ASME Journal of Pressure Technology Vol. 102, May 1980, pp. 188-193.

23. Kyriakides, S., and Babcock, C.D., 'Experimental Determination of the Propagation Pressure of Circular Pipes," Journal of Pressure Technology Vol. 103, pp. 326-336, Nov. 1981.

24. Hayes, D.J., and Manfred, D.L., 'Full Scale Crack Arrest Test and Arrestor Device Performance for the Flags Gasline," SPE 8220, 54th Annual Conference of SPE, Sept. 1979.

25. Walker, D.B.L., "A Technical Review of the Forties Field Submarine Pipeline," OTC 2603, pp. 819-829, May, 1976.

26. Lentini M., and Pereyra, V., "An Adaptive Finite Difference Solver for Nonlinear Two-Point Boundar Value Problems with Mild Boundary Layer," SIAM J. Numerical Analysis, Vol: 14, pp. 91-111.

27. Arbocz, J., "On the Problem of Limit Point Calculations," GALCIT SM 75-7, California Institute of Technology, 1975.

NOMENCLATURE

D	Pipe Mean Diameter
D_{max}	See Fig. 14
D_{min}	See Fig. 14
d	See Fig. 45
E	Young's Modulus
$\bar{E}$	Strain Hardening Modulus
E'	Arrestor Modulus
G	Arrestor Gap
h	Arrestor Thickness
H	Horizontal Force
$\bar{H}$	$3\pi H R/\sigma_o t^2$
K	Normalized Curvature, κ/κ_o
L	Arrestor Length
M	Bending Moment
M_o	$\sigma_o t^2/6$
$\bar{M}$	M/M_o
M_m^e	Pipe Elastic Limit Moment, $.987 \frac{E}{\sqrt{(1-\nu^2)}} Rt^2$
P	Pressure
P_c	Buckling Pressure
P_I	Initiation Pressure
P_p	Propagation Pressure
Q	$3\pi^2 PR^2/2\sigma_o t^2$
R	Pipe Radius, $D/2$
S	Mid-Plane Coordinate
s	$2S/\pi R$
t	Pipe Thickness

$\underline{u}$	Vector $(\bar{H}, \bar{V}, \bar{M}, \vartheta)$
V	Vertical Force
$\bar{V}$	$3\pi VR/\sigma_o t^2$
w_o	Amplitude of Initial Imperfection
(x,y)	Cartesian Coordinates
$(\bar{x}, \bar{y})$	$2(x,y)/\pi R$
Δ	Displacement of Ring at $\bar{y}$ (1)
ε	Strain
ε_o	Yield Strain, 5×10^{-3}
η	Arrestor Efficiency
ϑ	Angle (see Fig. 46)
ϑ_c	Bend Angle
κ	Curvature
κ_o	Curvature at First Yield
κ_m^e	Pipe Elastic Limit Curvature, $.493 \frac{E}{\sqrt{1-\nu^2}} Dt^2$
ν	Poisson's Ratio
σ	Stress
σ_o	Yield Stress
σ_o	Arrestor Yield Stress

TABLE 1. INITIATION PRESSURE TEST **PIPES**

PIPE	MATERIAL (STEEL)	DIAMETER (IN.)	THICKNESS (IN.)	D/T	P_P (PSI)
1	1018	1.250	.038	32.9	380
2	1018	1.375	.038	36.2	275
3	1010	1.500	.035	42.9	198
4	1018	5.252	.121	43.4	207'

• Calculated

TABLE 2. INDENTOR GEOMETRY

POINT INDENTOR #	DIAMETER (in.)	KNIFE INDENTOR #	DIAMETER (in.)
1	0.250	1	0.094
2	0.281	2	0.500
3	0.375	3	0.688
4	0.500	4	1.000
5	0.625	5	1.250

TABLE 3. INITIATION PRESSURE TEST DATA

PIPE #	INDENTOR #	P_I	D_{max}	D_{min}
1	p-2	1395	1.208	1.174
1	p-2	1158	1.303	1.119
1	p-2	887	1.340	1.044
1	p-2	733	1.387	0.969
2	p-2	1517	1.404	1.330
2	p-2	1244	1.395	1.291
2	p-2	952	1.416	1.242
2	p-2	742	1.450	1.156
2	P-1	725	1.470	1.156
2	p-2	716	1.467	1.145
2	P-3	695	1.474	1.143
2	P-4	687	1.500	1.106
2	P-5	674	1.499	1.121
2	P-5	668	1.512	1.096
2	P-4	646	1.490	1.119
2	p-2	577	1.590	0.966
2	p-2	570	1.555	1.023
2	p-2	489	1.595	0.947
2	p-2	456	1.729	0.818
2	p-2	374	1.094	0.864
2	k-1	1370	1.390	1.290
2	k-1	1026	1.422	1.240
2	k-1	790	1.408	1.102
2	k-3	791	1.457	1.163
2	k-2	780	1.468	1.158
2	k-5	735	1.484	1.126
2	k-4	724	1.480	1.132
2	k-1	706	1.480	1.139
2	k-1	649	1.544	0.998
2	k-1	532	1.671	0.891
2	k-1	466	1.756	0.796
2	k-1	434	1.747	0.822
2	k-1	425	1.761	0.806
2	k-1	379	1.783	0.787
3	p-2	662	1.536	1.362
3	p-2	496	1.609	1.223
3	p-2	394	1.727	1.071
3	p-2	333	1.869	0.893
3	p-2	270	1.888	0.918
3	k-1	596	1.558	1.334
3	k-1	446	1.664	1.173
3	k-1	330	1.851	0.948
3	k-1	310	1.890	0.914

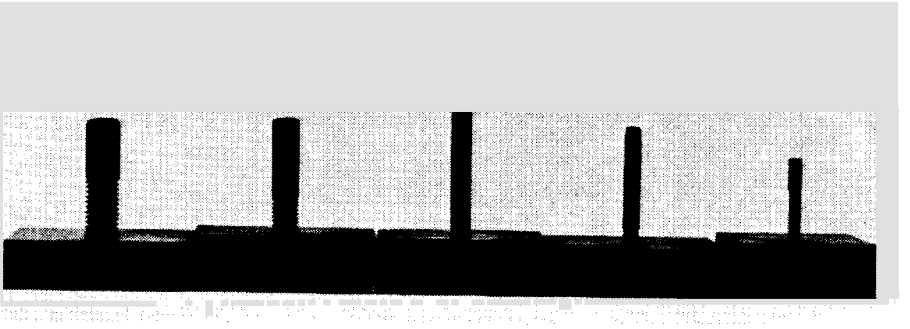

FIG. 1 "POINT" INDENTORS FOR INITIATION PRESSURE EXPERIMENTS

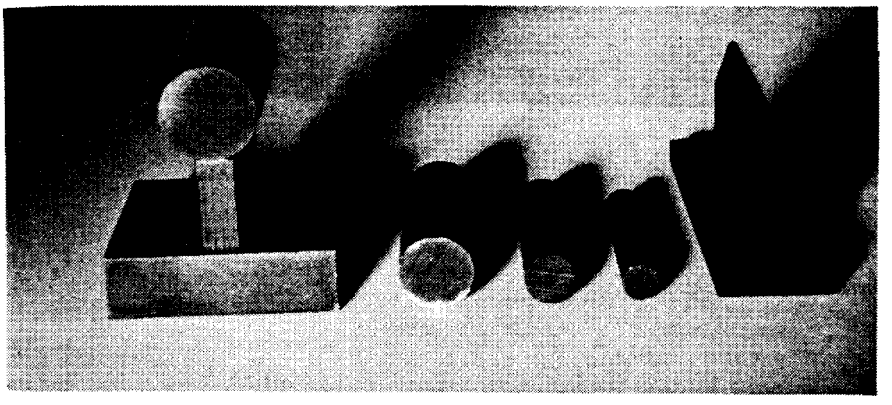

FIG. 2 "KNIFE EDGE" INDENTORS FOR INITIATION PRESSURE EXPERIMENTS

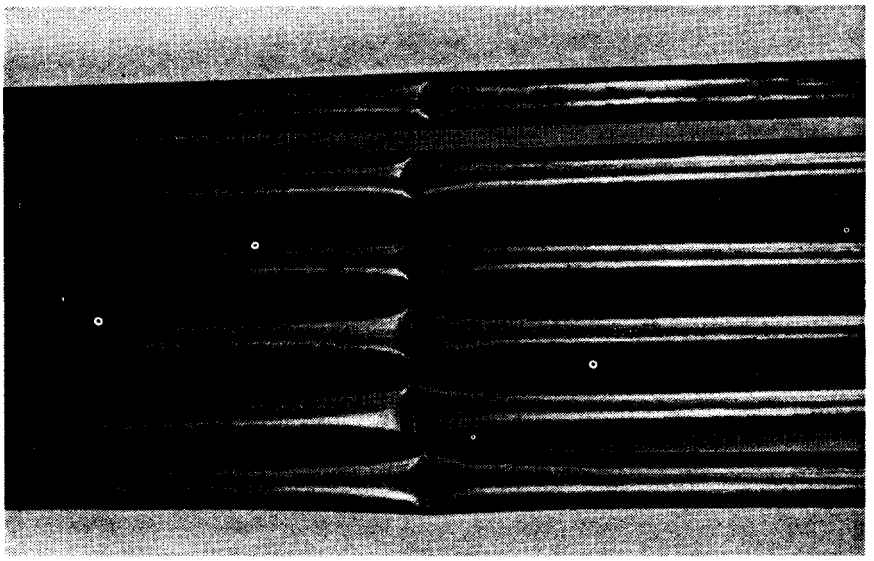

FIG. 3 RANGE OF "KNIFE EDGE" INDENTOR DAMAGE

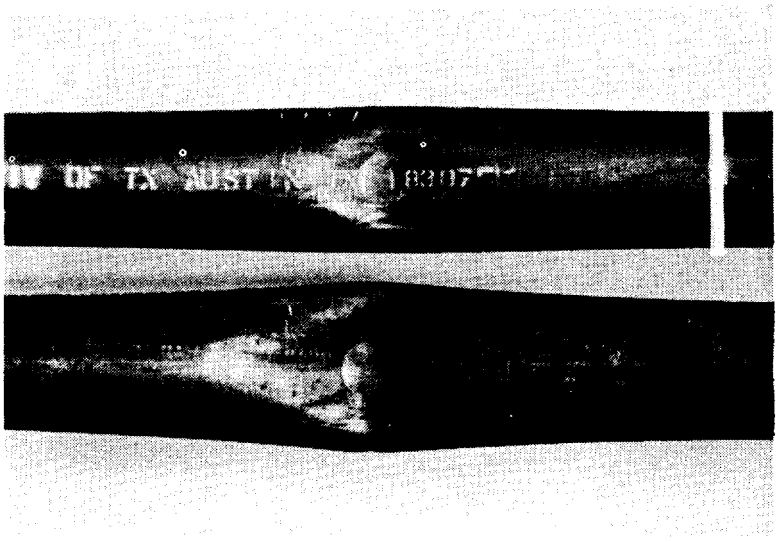

FIG. 4 "POINT" DAMAGE ON PIPE

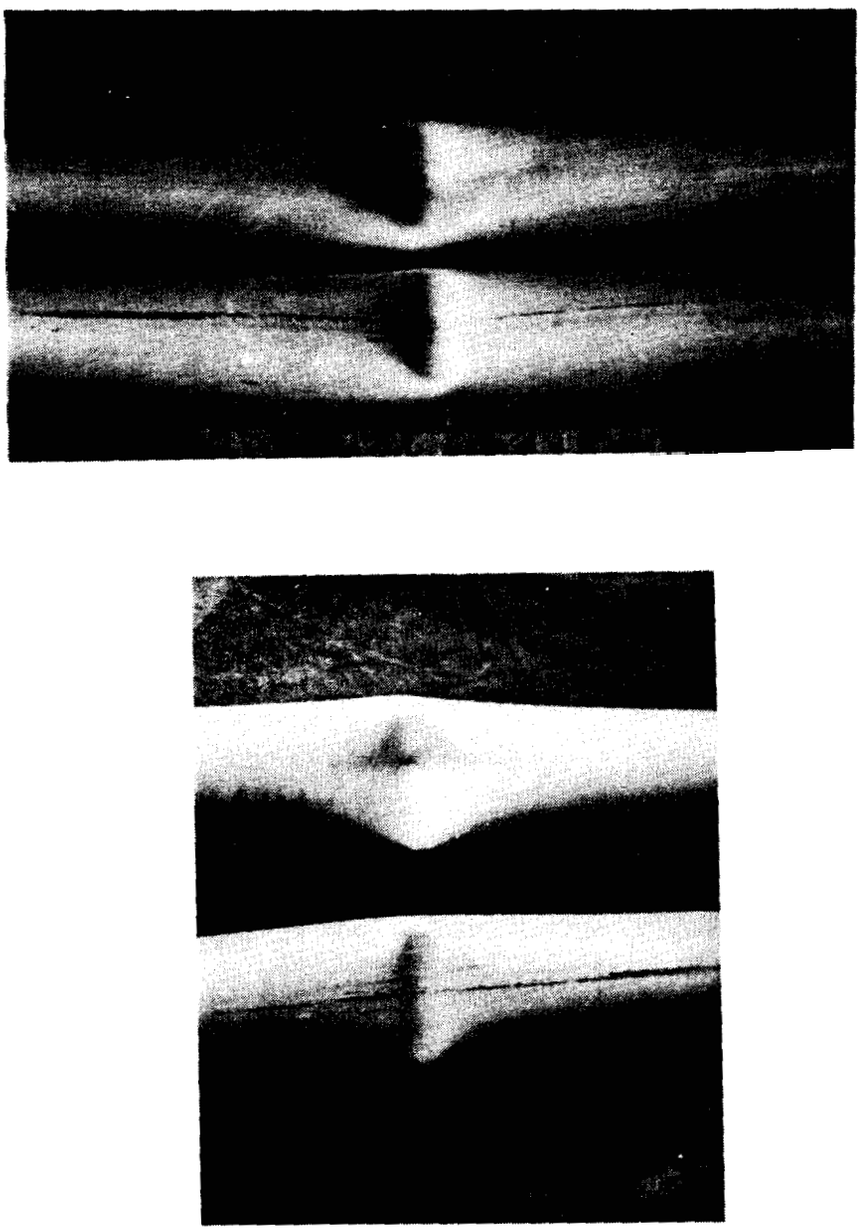

FIG. 5 **COMPARISON** OF "KNIFE EDGE" AND "POINT" DAMAGE

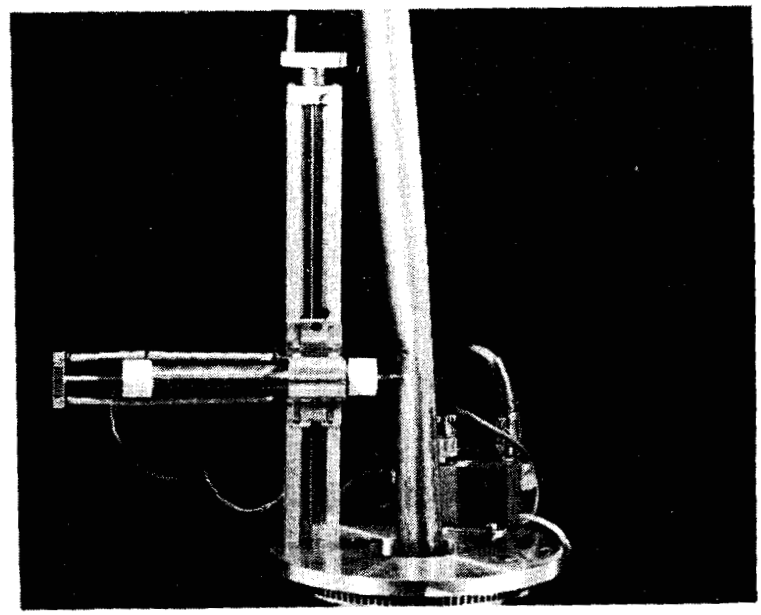

FIG. 6 IMPERFECTION SCANNING SYSTEM

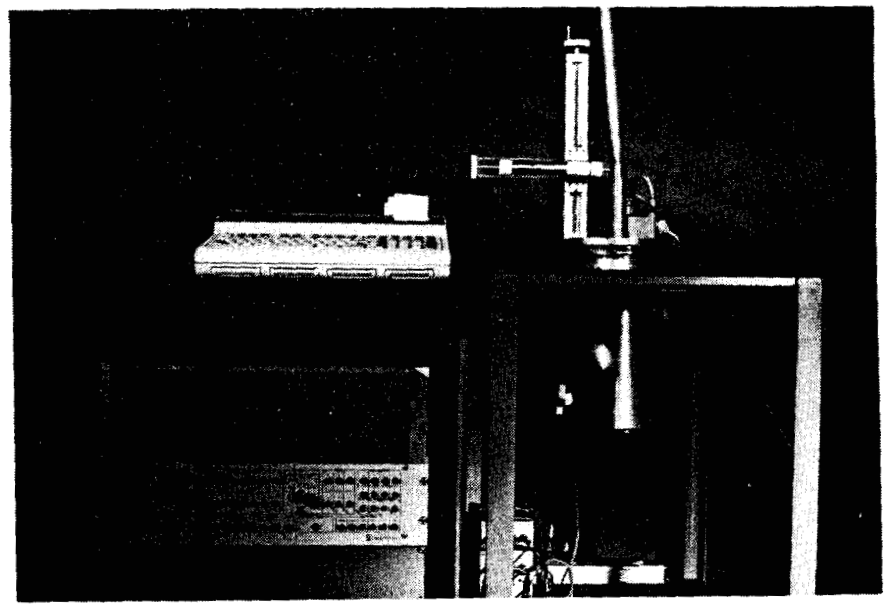

FIG. 7 IMPERFECTION **MEASURING** DEVICE WITH **DATA** ACQUISITION SYSTEM

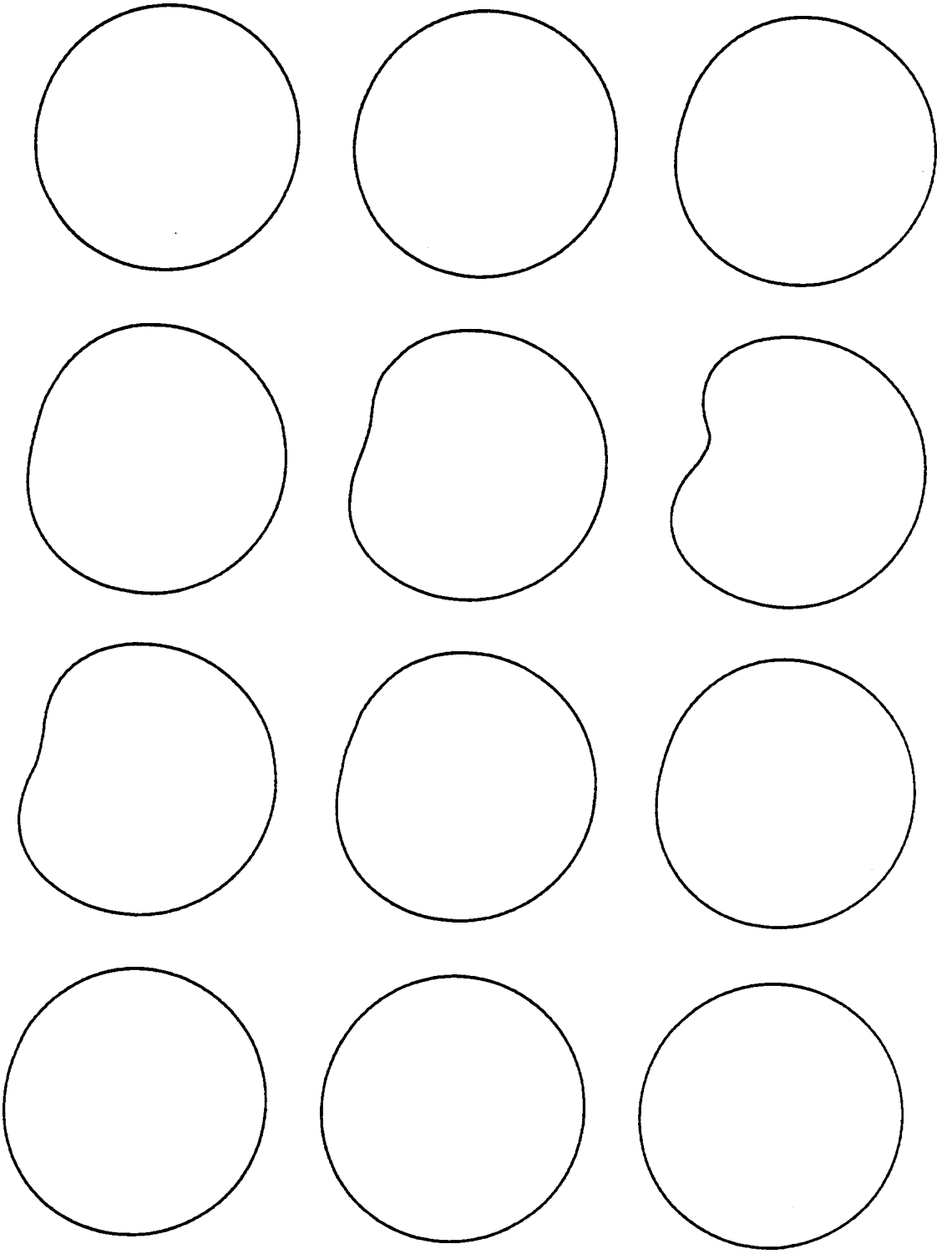

PIPE CROSS SECTIONS – MODERATE POINT DAMAGE

FIG.8

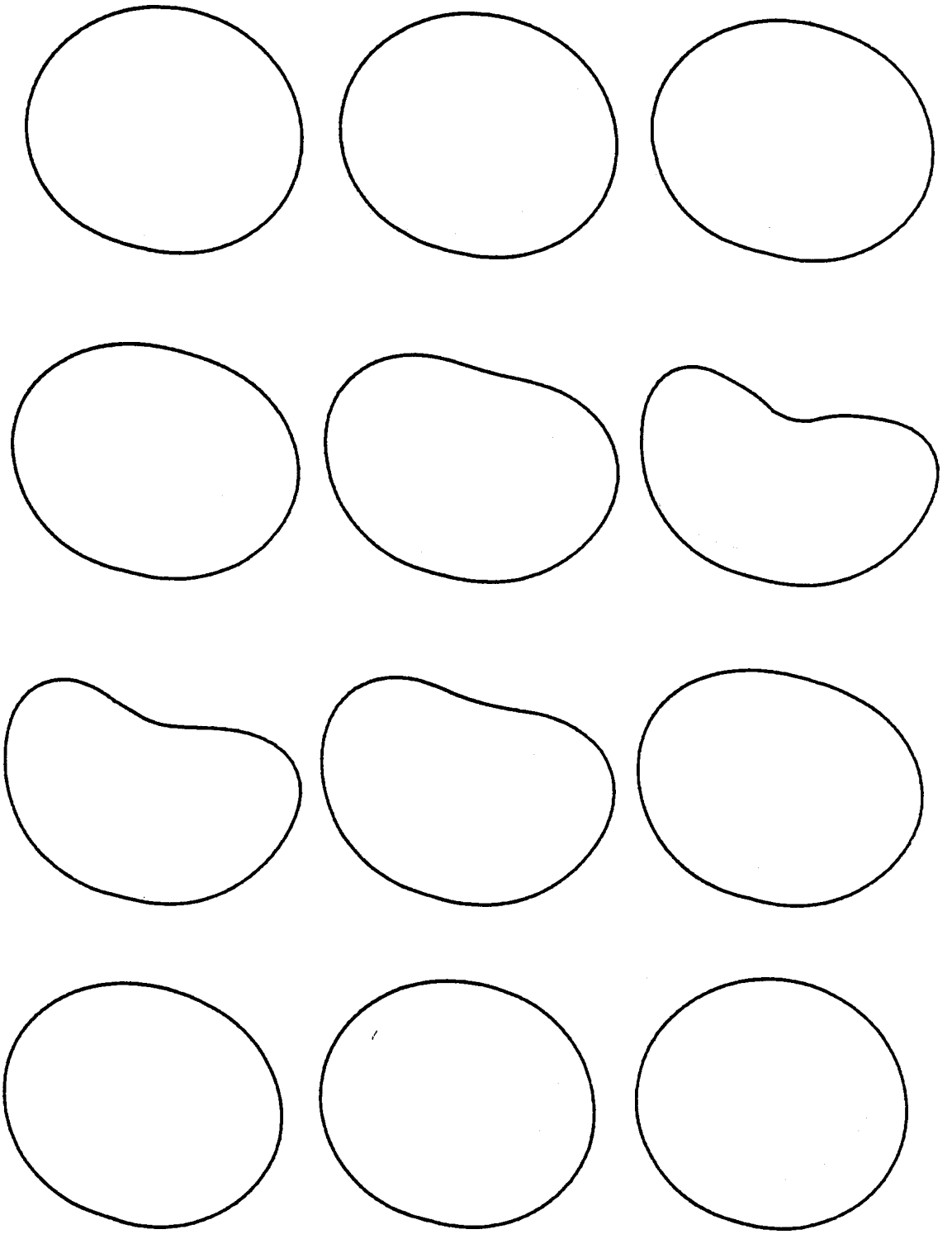

PIPE CROSS SECTIONS - SEVERE POINT DAMAGE

FIG.9

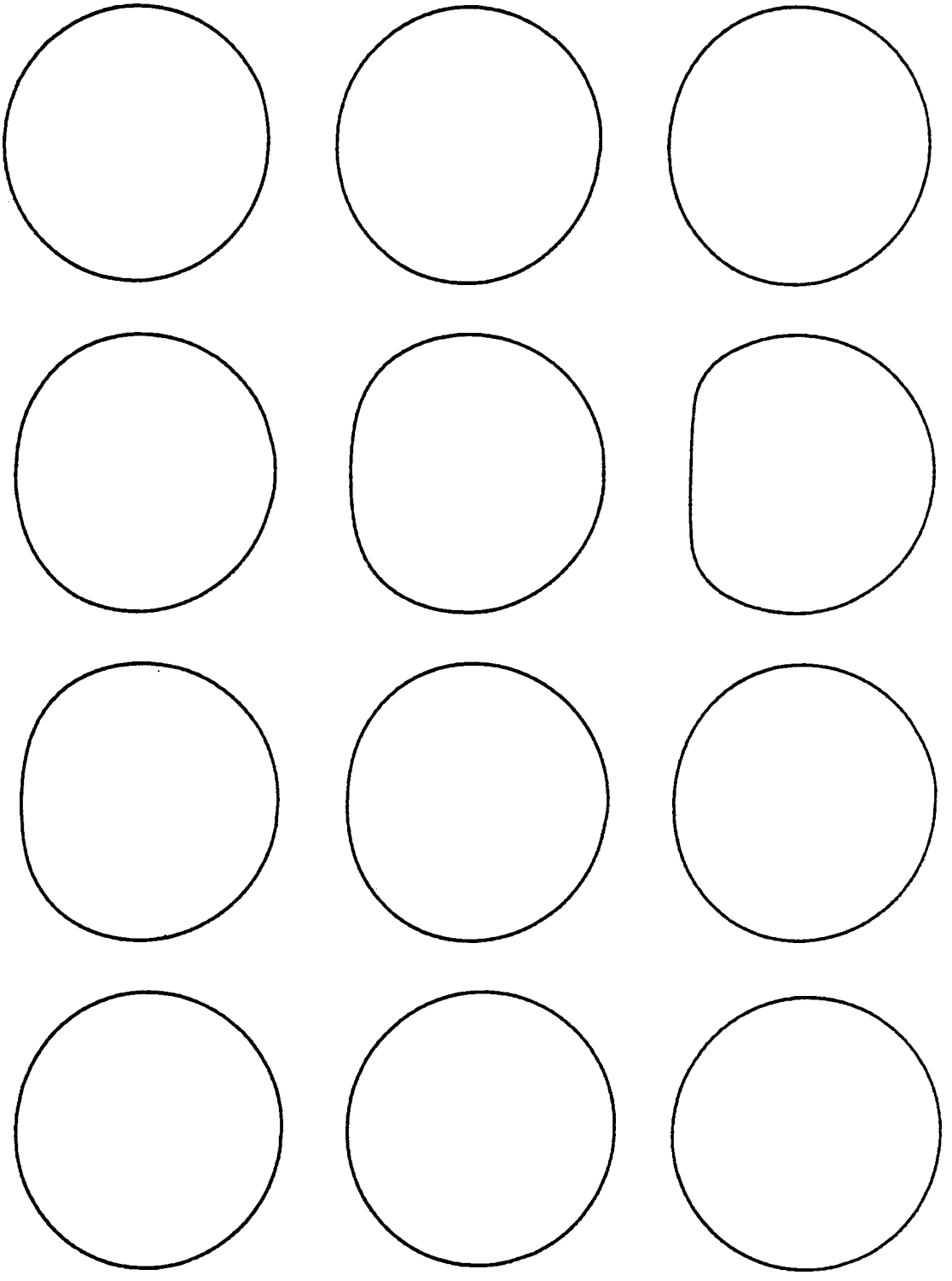

PIPE CROSS SECTIONS-MODERATE KNIFE EDGE DAMAGE

FIG.IO

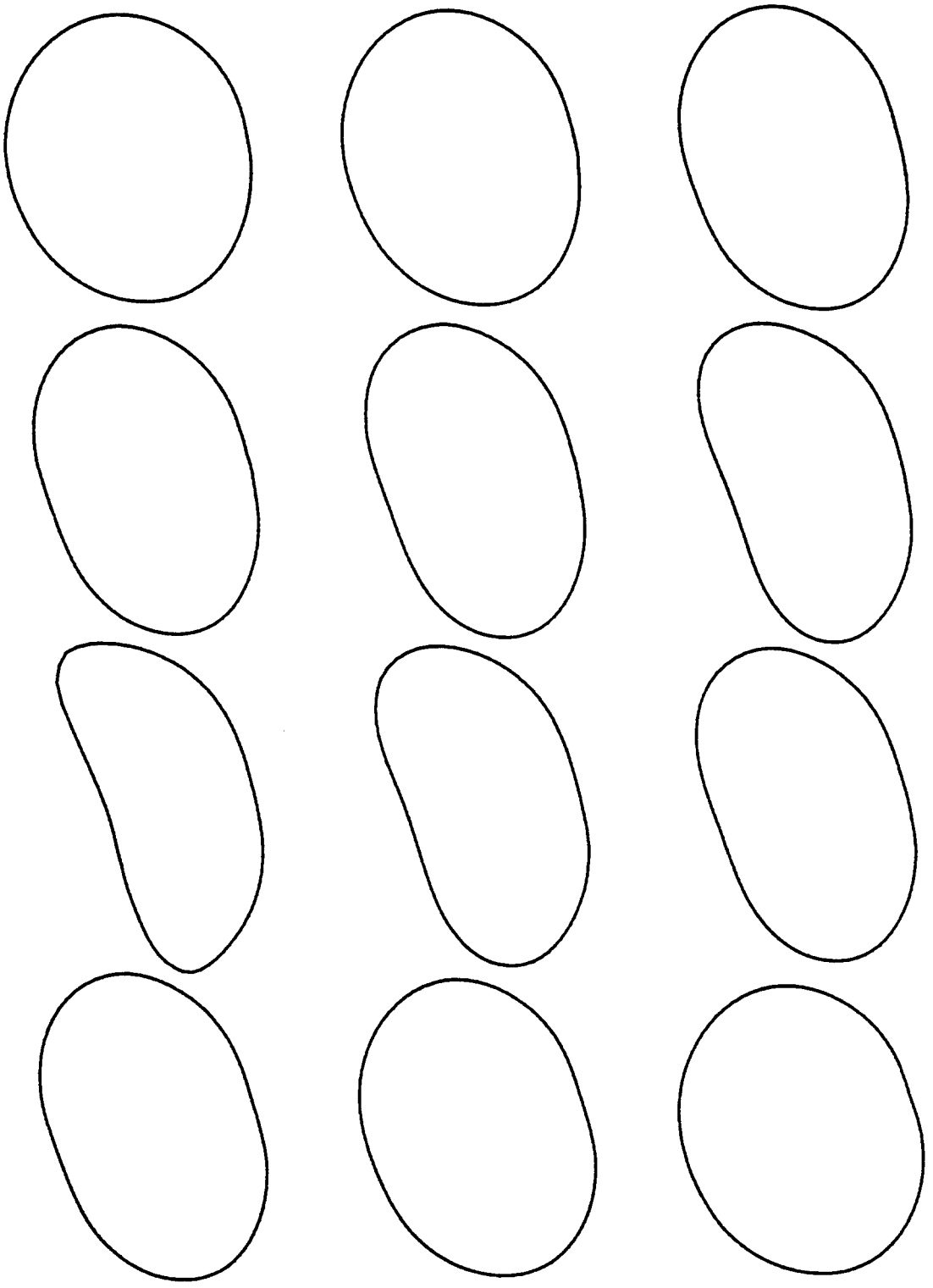

PIPE CROSS SECTIONS–SEVERE KNIFE EDGE DAMAGE

FIG. 11

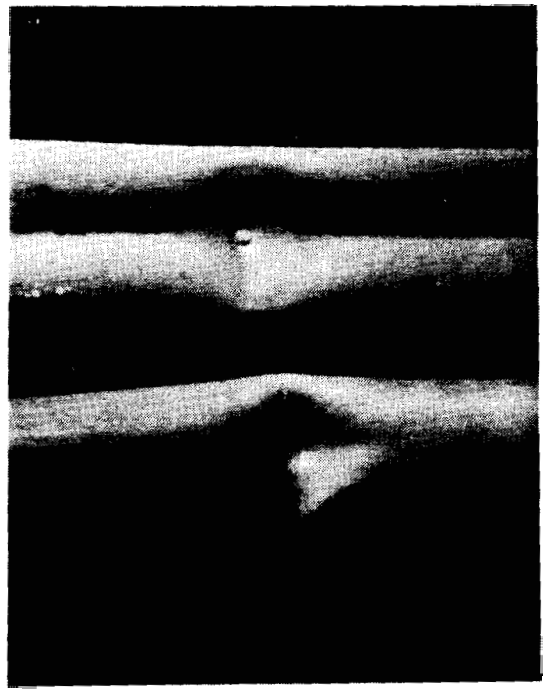

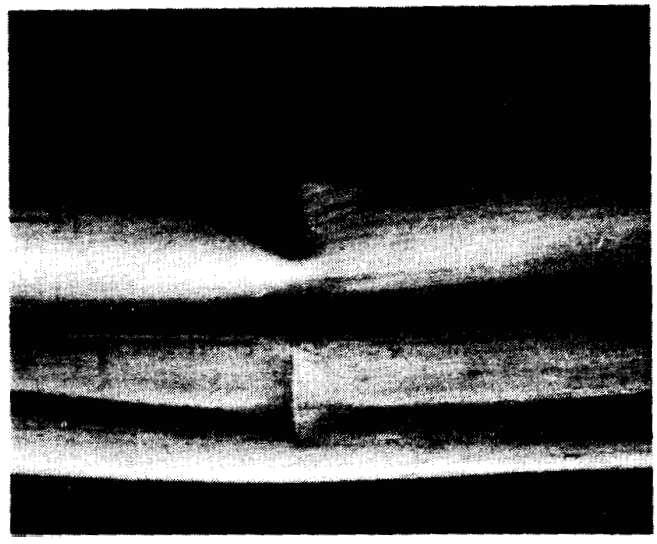

FIG. 12 PROPAGATING BUCKLE **AS** INITIATED FROM "POINT" AND "KNIFE EDGE" DAMAGE